Role of nitrogen vacancies in the luminescence of Mg-doped GaN

Qimin Yan, Anderson Janotti, Matthias Scheffler, and Chris G. Van de Walle

Role of nitrogen vacancies in the luminescence of Mg-doped GaN

Qimin Yan,[1] Anderson Janotti,[1] Matthias Scheffler,[1,2] and Chris G. Van de Walle[1]
[1]*Materials Department, University of California, Santa Barbara, California 93106-5050, USA*
[2]*Fritz-Haber-Institut der Max-Planck-Gesellschaft, Faradayweg 4–6, D-14195 Berlin, Germany*

Defects may cause compensation or act as recombination centers in Mg-doped GaN. Using hybrid functional calculations, we investigate the effects of nitrogen vacancies (V_N) and Mg-vacancy complexes (Mg_{Ga}-V_N) on the electrical and optical properties of GaN. We find that Mg_{Ga}-V_N are compensating centers in p-type but electrically inactive in n-type GaN. They give rise to a broad emission at 1.8 eV, explaining the red luminescence that is frequently observed in Mg-doped GaN, regardless of the Fermi level. Nitrogen vacancies are also compensating centers in p-type GaN and likely contribute to the yellow luminescence that has been observed in Mg-doped GaN. © *2012 American Institute of Physics*. [http://dx.doi.org/10.1063/1.3699009]

As GaN-based semiconductor devices are pushed to higher efficiencies, it becomes imperative to minimize the impact of defects that are detrimental to the device performance. In particular, it is crucial to understand the behavior and grasp control of defects that limit *p*-type doping by acting as recombination centers in Mg-doped GaN. It has been suggested that native defects such as nitrogen vacancies play an important role as compensating centers in *p*-type GaN.[1,2] Recent experiments based on positron annihilation spectroscopy (PAS) indicate the presence of nitrogen vacancies and their pairing with Mg impurities in Mg-doped GaN layers.[1,3] Since nitrogen vacancies are expected to induce deep levels in the band gap, they are also likely to affect the luminescence properties of GaN.

Conspicuous broad peaks in the yellow, blue, and red have been observed in the photoluminescence (PL) spectra of GaN layers synthesized under various growth conditions.[4–11] Yellow luminescence in *n*-type GaN has been attributed to Ga vacancies[12] and to C substituting on a N site in carbon-containing samples[13] but has also been observed in *p*-GaN.[10,11] The blue luminescence has often been attributed to recombination between a deep donor and a Mg acceptor.[14] The red PL band, with a peak position around 1.8 eV, has been observed in both *p*- and *n*-type GaN,[14] but its origins are unknown.

Based on the measurements of optically detected magnetic resonance (ODMR) in Mg-doped GaN, Bayerl *et al.* suggested that the red PL originates from recombination between a shallow donor and a deep acceptor,[5,6] with the deep level being related to V_N.[6] On the other hand, based on a correlation between the PAS spectrum, PL, and ODMR signals in such material, Zeng *et al.* concluded that the red PL originates from a deep donor to a deep acceptor transition, possibly related to V_N and Mg_{Ga}.[3] Density functional theory (DFT) calculations for the electronic properties of nitrogen vacancies and related complexes in GaN have also been reported.[2,15] However, the severe underestimation of band gaps in DFT precludes a direct comparison of the calculated defect levels with the observed luminescence peaks.

Here, we use a hybrid functional[16,17] approach that produces more accurate predictions for energetics and electronic structure of defects in semiconductors.[13] In this paper, we calculate the formation energies of V_N, Mg_{Ga}, and Mg_{Ga}-V_N

complexes in GaN, discuss all possible charge states, and determine optical absorption and emission energies from the calculated configuration-coordinate diagrams. We find that Mg_{Ga}-V_N complexes give rise to broad emission peaks at ∼1.8 eV explaining the experimental observations of the red PL in Mg-containing GaN. We also find that V_N can give rise to yellow luminescence in *p*-type GaN. The width of the emission peaks is a direct consequence of the large lattice relaxations for the different charge states of the defects (Fig. 1). Both Mg_{Ga}-V_N and V_N act as compensating centers in *p*-type GaN.

Our calculations are based on the generalized Kohn-Sham theory,[18] projector augmented wave (PAW) potentials,[19,20] and the screened hybrid functional of Heyd, Scuseria, and Ernzerhof (HSE),[16,17] as implemented in the VASP code.[21] The mixing parameter for the Hartree-Fock exchange potential is set to 31% (the original HSE value is 25%) in order to reproduce the experimental band gap of 3.5 eV. The calculated equilibrium lattice parameters of GaN, $a = 3.19$ Å and $c = 5.20$ Å, also agree well with experimental data ($a = 3.189$ Å and $c = 5.185$ Å at 300 K).[22] The defects are simulated using a 96-atom supercell, a cutoff of 300 eV for the plane-wave basis set, and a $2 \times 2 \times 2$ k-point mesh for the integrations over the Brillouin zone.

The electronic structure of V_N in GaN can be understood as follows. The removal of a N atom results in four Ga dangling bonds that, in the neutral charge state, are occupied by a total of three electrons. In the near-tetrahedral environment of the wurtzite structure, these dangling bonds combine into a symmetric state (*s*-like symmetry) near midgap, and three almost degenerate states (*p*-like symmetry) near the conduction band minimum (CBM). In the neutral defect, the lower state in the gap is occupied by two electrons, and the third electron occupies the lowest of the three states near the CBM. From this picture, it emerges that +, 2+, and 3+ charge states may be obtained by successively removing electrons from the V_N Kohn-Sham defect states. Similarly, negative charge states can in principle be obtained by adding electrons, but electron-electron repulsion will push the states upwards, i.e., closer to the CBM. Atomic relaxations will of course affect the positions of the Kohn-Sham states; whether a particular charge state is actually thermodynamically stable
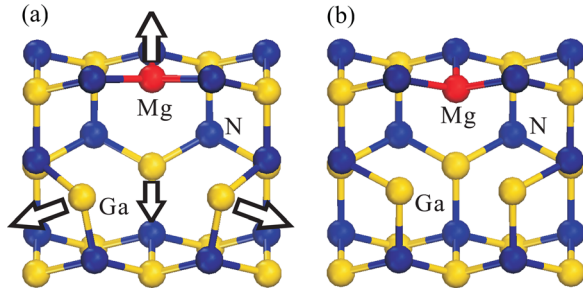
FIG. 1. Geometry of (a) the $(Mg_{Ga}\text{-}V_N)^{2+}$ and (b) the $(Mg_{Ga}\text{-}V_N)^0$ complexes in GaN.

thus needs to be determined on the basis of its formation energy.

The Mg_{Ga} acceptor in neutral charge state, on the other hand, introduces a state near the valence band maximum (VBM) that is singly occupied. The association of V_N with Mg_{Ga} will result in an electron being transferred from a V_N state to the Mg_{Ga}-acceptor state. The Mg_{Ga} will also perturb the position of the vacancy-induced gap states. The geometry of the $Mg_{Ga}\text{-}V_N$ complex is shown in Fig. 1.

The formation energies of V_N, Mg_{Ga}, and the $Mg_{Ga}\text{-}V_N$ complex are given by

$$E^f(V_N^q) = E_t(V_N^q) - E_t(\text{GaN}) + \mu_N + q\epsilon_F + \Delta^q, \quad (1)$$

$$E^f(Mg_{Ga}^q) = E_t(Mg_{Ga}^q) - E_t(\text{GaN}) + \mu_{Ga} - \mu_{Mg} + q\epsilon_F + \Delta^q, \quad (2)$$

$$E^f[(Mg_{Ga}\text{-}V_N)^q] = E_t[(Mg_{Ga}\text{-}V_N)^q] - E_t(\text{GaN})$$
$$- \mu_{Mg} + \mu_{Ga} + \mu_N + q\epsilon_F + \Delta^q, \quad (3)$$

where $E_t(V_N^q), E_t(Mg_{Ga}^q)$, and $E_t[(Mg_{Ga}\text{-}V_N)^q]$ are the total energies of the supercells containing V_N, Mg_{Ga}, and the $Mg_{Ga}\text{-}V_N$ complex in charge state q, and $E_t(\text{GaN})$ is the total energy of a perfect crystal in the same supercell.

The N atom removed from the crystal is placed in a reservoir of energy μ_N, and the Ga atom that is removed is placed in a reservoir of energy μ_{Ga}. The chemical potentials μ_N and μ_{Ga} can vary over a range determined by the calculated GaN formation enthalpy $[\Delta H_f(\text{GaN}) = -1.34 \text{ eV}]$, reflecting growth conditions that can vary from N-rich to Ga-rich. The Mg atom that is added is taken from a reservoir with energy μ_{Mg}. We assume that the chemical potential of Mg is limited by the formation of Mg_3N_2, with a formation enthalpy of $\Delta H_f(Mg_3N_2) = -4.8 \text{ eV}$, then the upper limit of Mg chemical potential is determined by $3\mu_{Mg} + 2\mu_N = \Delta H_f(Mg_3N_2)$. Note that the formation energy of V_N is lower under Ga-rich conditions.

In the case of charged defects, electrons are exchanged with the reservoir for electrons in the solid, the energy of which is the Fermi level ϵ_F, referenced to the VBM. The last term, Δ^q, is the correction for charged defects due to the finite size of the supercell, as described in Ref. 23. For instance, for V_N, we obtain Δ^q values 0.13 eV, 0.61 eV, and 1.46 eV for $q = +1$, 2+, and 3+ charge states, respectively.

The formation energies for the nitrogen vacancy and the $Mg_{Ga}\text{-}V_N$ complex are shown in Fig. 2. Both $Mg_{Ga}\text{-}V_N$ and V_N

have low formation energies and are stable as donors when the Fermi level is near the VBM. This indicates that these defects can play an important role as compensating centers in *p*-GaN.

Figs. 2(a) and 2(b) show that V_N is most stable in the 3+ charge state for Fermi-level positions near the VBM. The thermodynamic level corresponding to the transition between the 3+ and + states occurs at 0.47 eV above the VBM. The 2+ charge state is always higher in energy than the + and 3+ charge states, forming a negative-U center. In *n*-type GaN, in which ϵ_F is close to the CBM, the formation energy of V_N is very high, indicating it is unlikely to form. A transition between + and neutral charge states occurs at 0.24 eV below the CBM. We find that the negative charge state is not stable for Fermi-level positions within the band gap. Note that if the band gap is corrected by a scissor operator,[24] negative charge states are stabilized.

The negative-U character, in which the 2+ charge state is always higher in energy than the 3+ and + states, is due to large and charge-state dependent relaxations around V_N. The four nearest-neighbor Ga atoms relax away from the vacancy by 1.1%, 10.8%, and 21.9% of the equilibrium Ga-N bond length for the +, 2+, and 3+ charge state, respectively. In the neutral and negative charge states, the Ga atoms surrounding the vacancy pair up and move inward, with Ga-Ga distances of 2.96 Å within each pair for V_N^0 and 2.70 Å for V_N^-, significantly smaller than the Ga-Ga distances around the vacancy in the + charge state (3.23 Å).

Since Mg is an acceptor and V_N is a donor in GaN, we expect them to attract and form a complex. We find the stable charge states of the $Mg_{Ga}\text{-}V_N$ complex to be 2+, +, and neutral. The 2+/+ transition level occurs at 0.84 eV above the VBM, and the +/0 level at 0.89 eV. Therefore, the 2+
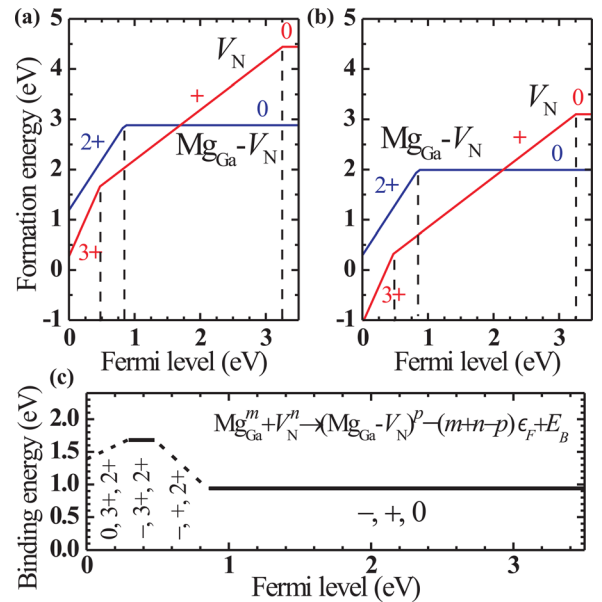

FIG. 2. Formation energies as a function of Fermi level for the nitrogen vacancy V_N and the $Mg_{Ga}\text{-}V_N$ complex in GaN, under (a) N-rich and (b) Ga-rich conditions. (c) Binding energies (E_B) as a function of Fermi level. In each region of Fermi level, we only take into account the defect and complex charge states with lowest formation energies and their charge states (m, n, p) are listed. The solid lines indicate processes where the charge neutrality condition is fulfilled, while the dashed lines indicate processes that require exchange of carriers with the Fermi level and may involve additional barriers.

state is stable in *p*-type, while the neutral state is stable in *n*-type GaN. As shown in Fig. 2(c) as solid lines, the binding energy (E_B) for the $(Mg_{Ga}\text{-}V_N)^0$ complex with respect to dissociation into Mg_{Ga}^- and V_N^+ is 0.94 eV, while that for $(Mg_{Ga}\text{-}V_N)^{2+}$ with respect to Mg_{Ga}^- and V_N^{3+} is 1.69 eV. There are two other dissociation processes that require exchange of carriers with the band edges and hence depend on the Fermi level position: the dissociation of $(Mg_{Ga}\text{-}V_N)^{2+}$ into Mg_{Ga}^0 and V_N^{3+}, and the dissociation of $(Mg_{Ga}\text{-}V_N)^{2+}$ into Mg_{Ga}^- and V_N^+. The first requires the release of an electron, and the binding energy thus increases with Fermi level. The second requires the capture of electrons, and the binding energy decreases with the Fermi-level position. Note that these two processes may involve additional barriers due to the necessity for carrier exchange with the bulk.

The local lattice relaxations for the $(Mg_{Ga}\text{-}V_N)^0$ and $(Mg_{Ga}\text{-}V_N)^{2+}$ complexes are illustrated in Fig. 1. The three nearest-neighbor Ga atoms are displaced away from the vacancy by 21% and 9.5% of the equilibrium Ga-N bond length in the 2+ and + charge states, while in the neutral charge state, they relax towards the vacancy by 1.2%; the Mg atom relaxes away from the vacancy by 20.1%, 10.0%, and 4.7% in the 2+, +, and neutral charge states, respectively.

Given that V_N and $Mg_{Ga}\text{-}V_N$ are deep centers in GaN, they likely lead to characteristic absorption and emission peaks. The charge-state dependent local lattice relaxations of the different charge states will lead to significant Stokes shifts and strong vibrational broadening of those peaks. The optical transition energies are determined from the calculated configuration-coordinate diagrams shown in Fig. 3. The energy difference between minima in the configuration-coordinate diagram corresponds to the zero-phonon line and is equal to the difference between the $q/q+1$ transition level and the CBM (Fig. 2). For the $Mg_{Ga}\text{-}V_N$ complex, we identify two processes by which emission can be observed in PL experiments, depending on the Fermi level position.

In *p*-type GaN [Fig. 3(a)], where Mg doping is intentional, the $Mg_{Ga}\text{-}V_N$ complex is stable in the 2+ charge state. During the photoluminescence process, an electron previously excited from the valence band to the conduction band can make a transition to the empty defect state of $(Mg_{Ga}\text{-}V_N)^{2+}$, i.e., $(Mg_{Ga}\text{-}V_N)^{2+} \rightarrow (Mg_{Ga}\text{-}V_N)^+$. The absorption energy in this case is the band-gap energy. The peak emission energy

corresponds to the energy difference between $(Mg_{Ga}\text{-}V_N)^{2+}$ and $(Mg_{Ga}\text{-}V_N)^+$ in the lattice configuration corresponding to the initial configuration, i.e., that of $(Mg_{Ga}\text{-}V_N)^{2+}$. From our calculations, this results in an emission peak at 1.83 eV, with a relaxation energy of 0.83 eV as shown in Fig. 3(a). Our results thus indicate that $Mg_{Ga}\text{-}V_N$ is a source of red luminescence in *p*-type GaN, explaining the experimental observations of the red PL.[6,7]

In the case of *n*-type GaN, in which Mg may be present unintentionally or due to intentional co-doping, the $Mg_{Ga}\text{-}V_N$ complex occurs in the neutral charge state (Fig. 2). An electron can be excited from the defect state to the conduction band, with a peak absorption energy of 3.33 eV, given by the energy difference between $(Mg_{Ga}\text{-}V_N)^0$ and $(Mg_{Ga}\text{-}V_N)^+$, both in the lattice configuration corresponding to the initial neutral charge state. Emission will occur at 1.81 eV, corresponding to the energy difference between $(Mg_{Ga}\text{-}V_N)^+$ and $(Mg_{Ga}\text{-}V_N)^0$ in the lattice configuration of the positive charge state. Our results thus indicate that the $Mg_{Ga}\text{-}V_N$ complex can also lead to broad red luminescence in *n*-type GaN.[8,9]

Also isolated V_N can give rise to photoluminescence. We focus on *p*-type GaN, in which isolated V_N are most likely to occur and stable in the 3+ charge state (Fig. 2). An electron excited to the CBM can recombine with the empty defect state, resulting in a $V_N^{3+} \rightarrow V_N^{2+}$ transition. The corresponding emission peaks at 2.18 eV, which is in the yellow region of the spectrum, with a relaxation energy of 0.81 eV. We thus conclude that the isolated V_N center may be a source of yellow luminescence in *p*-type GaN, consistent with experimental observations.[10,11]

In summary, based on hybrid density functional calculations, we have shown that $Mg_{Ga}\text{-}V_N$ complexes lead to broad red luminescence in both *p*- and *n*-type GaN. We also find that isolated nitrogen vacancies can give rise to broad emission peaked at 2.18 eV. Our results provide an explanation for the mechanisms of the red and yellow luminescence signals that have been observed in Mg-containing GaN.
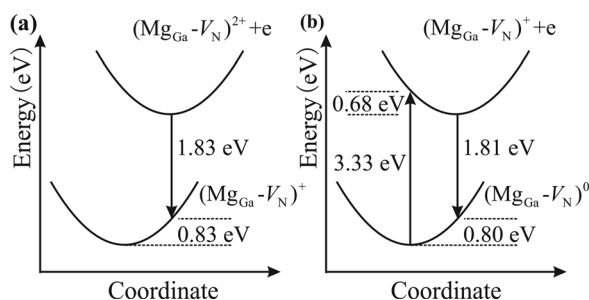
FIG. 3. Configuration-coordinate diagrams for the $Mg_{Ga}\text{-}V_N$ complex. (a) Illustration of the transition between an electron in the CBM (previously excited from the valence band) and the deep acceptor state related to $(Mg_{Ga}\text{-}V_N)^{2+}$ that leads to red luminescence (1.83 eV). (b) The $(Mg_{Ga}\text{-}V_N)^0$ to $(Mg_{Ga}\text{-}V_N)^+$ optical absorption starts at 2.61 eV and peaks at 3.33 eV, while the $(Mg_{Ga}\text{-}V_N)^+$ to $(Mg_{Ga}\text{-}V_N)^0$ emission peaks at 1.81 eV, in the red region of the spectrum.

[1]S. Hautakangas, J. Oila, M. Alatalo, K. Saarinen, L. Liszkay, D. Seghier, and H. P. Gislason, Phys. Rev. Lett. **90**, 137402 (2003).

[2]C. G. Van de Walle and J. Neugebauer, J. Appl. Phys. **95**, 3851 (2004).

[3]S. Zeng, G. N. Aliev, D. Wolverson, J. J. Davies, S. J. Bingham, D. A. Abdulmalik, P. G. Coleman, T. Wang, and P. J. Parbrook, Appl. Phys. Lett. **89**, 022107 (2006).

[4]S. Nakamura, N. Iwasaki, M. Senoh, and T. Mukai, Jpn. J. Appl. Phys. **31**, 1258 (1992).

[5]M. W. Bayerl, M. S. Brandt, E. R. Glaser, A. E. Wickenden, D. D. Koleske, R. L. Henry, and M. Stutzmann, Phys. Status Solidi B **216**, 547 (1999).

[6]M. W. Bayerl, M. S. Brandt, O. Ambacher, M. Stutzmann, E. R. Glaser, R. L. Henry, A. E. Wickenden, D. D. Koleske, T. Suski, I. Grzegory, and S. Porowski, Phys. Rev. B **63**, 125203 (2001).

[7]U. Kaufmann, M. Kunzer, H. Obloh, M. Maier, C. Manz, A. Ramakrishnan, and B. Santic, Phys. Rev. B **59**, 5561 (1999).

[8]W. Götz, L. T. Romano, B. S. Krusor, N. M. Johnson, and R. J. Molnar, Appl. Phys. Lett. **69**, 242 (1996).

[9]C. Lee, J.-E. Kim, H. Y. Park, S. T. Kim, and H. Lim, J. Phys.: Condens. Matter **10**, 11103 (1998).

[10]G. Salviati, N. Armani, C. Zanotti-Fregonara, E. Gombia, M. Albrecht, H. P. Strunk, M. Mayer, M. Kamp, and A. Gasparotto, MRS Internet J. Nitride Semicond. Res. **5S1**, W11.50 (2000).

[11]O. Gelhausen, H. N. Klein, M. R. Phillips, and E. M. Goldys, Appl. Phys. Lett. **83**, 3293 (2003).

[12]J. Neugebauer and C. G. Van de Walle, Appl. Phys. Lett. **69**, 503 (1996).

[13]J. L. Lyons, A. Janotti, and C. G. Van de Walle, Appl. Phys. Lett. **97**, 152108 (2010).

[14]M. A. Reshchikov and H. Morkoç, J. Appl. Phys. **97**, 061301 (2005).

[15]F. A. Reboredo and S. T. Pantelides, Phys. Rev. Lett. **82**, 1887 (1999).

[16]J. Heyd, G. E. Scuseria, and M. Ernzerhof, J. Chem. Phys. **118**, 8207 (2003).

[17]J. Heyd, G. E. Scuseria, and M. Ernzerhof, J. Chem. Phys. **124**, 219906 (2006).

[18]W. Kohn and L. J. Sham, Phys. Rev. **140**, A1133 (1965).

[19]G. Kresse and D. Joubert, Phys. Rev. B **59**, 1758 (1999).

[20]P. E. Blöchl, Phys. Rev. B **50**, 17953 (1994).

[21]G. Kresse and J. Furthmüller, Phys. Rev. B **54**, 11169 (1996).

[22]O. Madelung, *Semiconductors-Basic Data*, 2nd revised ed. (Springer, Berlin, 1996).

[23]C. Freysoldt, J. Neugebauer, and C. G. Van de Walle, Phys. Rev. Lett. **102**, 016402 (2009).

[24]M. G. Ganchenkova and R. M. Nieminen, Phys. Rev. Lett. **96**, 196402 (2006).